UCRL- 84518
PREPRINT
CONF-801011--13

THE DESIGN OF TANDEM MIRROR REACTORS WITH THERMAL BARRIERS

Gustav A. Carlson

This paper was prepared for inclusion in the Proceedings of the Fourth ANS Topical Meeting on The Technology of Controlled Nuclear Fusion, King of Prussia, PA, October 14-17, 1980.

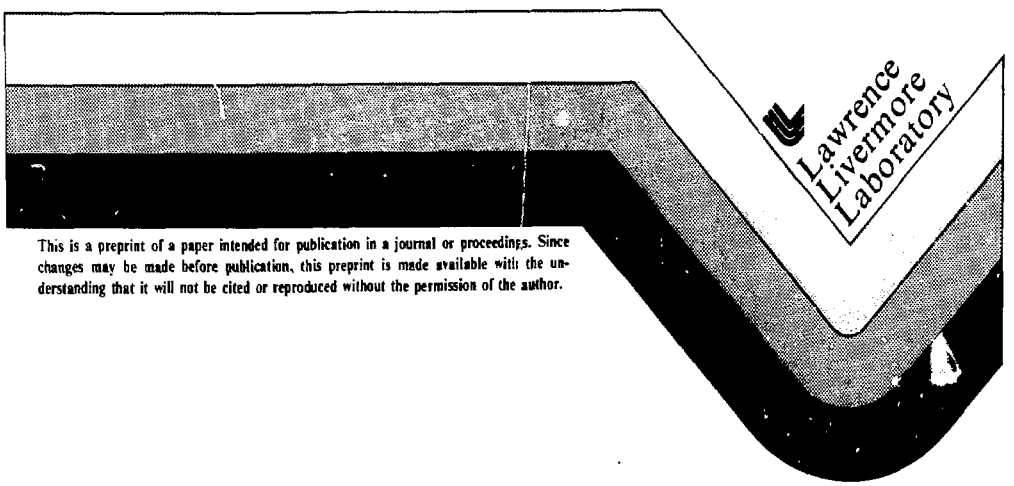

THE DESIGN OF TANDEM MIRROR REACTORS WITH THERMAL BARRIERS*

Gustav A. Carlson
Lawrence Livermore National Laboratory, University of California

In a tandem mirror fusion reactor, the fusion power is produced in the straight cylindrical central cell. The central-cell magnets are low-field solenoids. Because the central-cell plasma is near or at ignition, no plasma heating hardware is required for the central cell. A basic design philosophy for the central cell is that of axial modularity, and a number of different module designs have been proposed which lend themselves to mass-production techniques.

Axial confinement of the central-cell fusion plasma is enhanced by the electrostatic potential of the plug plasmas. The incorporation of thermal barriers (regions of depressed potential between the central cell and plug plasmas) allows the confining potential to be created partly by an elevated plug electron temperature instead of solely by a higher plug density. A number of different thermal barrier configurations have been proposed, and are now under comparative study. A primary concern is the determination of magnetic field shapes that will ensure magnetohydrodynamic (MHD) stability at high central-cell β.

End-plug technologies for tandem mirror reactors include high-field superconducting magnets, neutral beam injectors, and gyrotrons for electron cyclotron resonant heating (ECRH). In addition to their normal use for sustenance of the end-plug plasmas, neutral beam injectors are used for "pumping" trapped ions from the thermal barrier regions by charge exchange. An extra function of the axially directed pump beams is the removal of thermalized alpha particles from the reactor. The principles of tandem mirror operation with thermal barriers will be demonstrated in the upgrade of the Tandem Mirror Experiment (TMX-U) in 1981 and the tandem configuration of the Mirror Fusion Test Facility (MFTF-B) in 1984. Continued analysis and conceptual design over this period will evolve the optimal configuration and parameters for a power producing reactor.

*Work performed under the auspicies of the U.S. Department of Energy by the Lawrence Livermore National Laboratory under contract number W-7405-ENG-48.

Introduction

The tandem mirror confinement concept, invented in 1976 by Logan and Fowler[1] and independently by Dimov[2] in the USSR, is now the mainline effort of the mirror fusion program. The basic concept entails the improved axial confinement of a long cylindrical fusion plasma within a solenoid by means of strong electrostatic potentials at the ends, produced by mirror-confined, end-plug plasmas. Operation of the Tandem Mirror Experiment (TMX) at Lawrence Livermore National Laboratory has demonstrated the validity of the basic tandem mirror concept. The first conceptual fusion reactor design based on the concept was published in July 1977.[3] Drawbacks of the first design included a somewhat modest plasma performance (Q = fusion power/total injected power trapped by the plasma = 5) and a requirement for high-technology components for the end plugs (17-T magnetic coils and 1.2-MeV neutral-beam injectors).

A major new invention for tandem mirrors—the thermal barrier concept—was reported in April 1979.[4] This invention followed from the realization that the optimal use of electron heating in the tandem mirror involves the establishment of a hotter electron population in the plugs than in the central cell. However, in the normal tandem mirror, electron flow between the plugs and central cell is so high that only small temperature differences can be established, even with electron heating localized in the end plugs. The new concept introduces a barrier between the plug and central cell that effectively reduces the passing of central cell electrons into the plug. Basically, the thermal barrier consists of a region of much reduced magnetic field strength, plasma density, and plasma potential.

The thermal barrier principle will first be tested in an upgrade of the TMX facility, scheduled for completion by November 1981.[5] Plasma confinement in a large tandem mirror with thermal barriers will be explored in the tandem configuration of the Mirror Fusion Test Facility (MFTF-B), recently approved by DOE for construction at Lawrence Livermore National Laboratory (LLNL).[6] MFTF-B, which will incorporate the MFTF minimum-B mirror cell (already under con-

struction) as one end plug, is scheduled for completion by October 1984, and is predicted to achieve a D-T-equivalent Q near unity (only deuterium will be used in the experiment).

A preliminary conceptual design of a power reactor based on the tandem mirror with thermal barriers was reported in September 1979.[7] An overall view of the reactor is shown in Fig. 1.

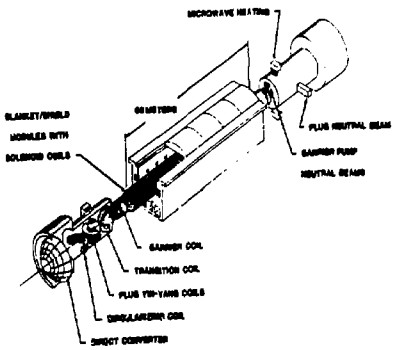

Fig. 1 Tandem mirror reactor with thermal barriers.

The D-T fusion plasma is contained in the 56-m-long central cell and produces 1770 MW of fusion power. With Q = 10, the reactor will produce about 500 MW of net electricity. Because the central-cell plasma is near or at ignition, the power output of the reactor can be increased by increasing the central cell length and retaining the same end plug systems. The central cell consists of 28 2-m-long modules, each containing an annular blanket region, a magnet shield region, and two niobium titanium solenoidal magnets. The end-plug magnets are housed in large cylindrical vacuum vessels at each end of the reactor. The plug plasmas are each sustained by a low-current, 400-keV neutral beam (shown only on the far end in Fig. 1). Also shown is the gyrotron tube system for microwave heating of the electrons on the plug side of the thermal barrier. The small neutral beams indicated on the end wall of the plug vacuum vessel are the barrier-region beams for charge-exchange pumping of the barrier and fueling of the central cell.

Since the publication of Ref. 7, the rapidly evolving knowledge concerning tandem mirrors with thermal barriers has resulted in a number of alternative end-plug configurations. The investigation and comparison of these different end plugs are the principal present efforts in the area of tandem mirror power reactor design. The remainder of this paper will describe the various end-plug configurations and also the design of the power-producing central cell for a typical tandem mirror reactor.

End Plug Configurations for Tandem Mirrors with Thermal Barriers

The main function of the thermal barrier is to thermally insulate the electrons in the end plug from contact with those in the solenoid. The concept is sketched in Fig. 2, which compares the plasma potential profiles in the

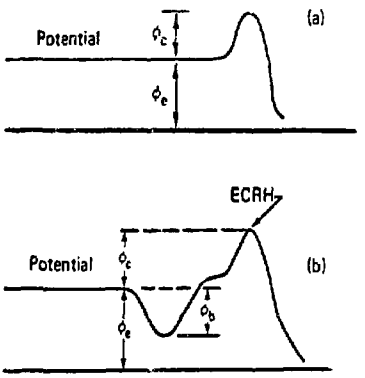

Fig. 2. Plasma potential profile for basic tandem mirror and for tandem mirror with thermal barriers.

neighborhood of an end plug for the basic tandem configuration and for the tandem mirror with thermal barriers. The new feature is a depression in the potential at the entrance to the end plug. This depression in the positive potential appears to the negatively charged electrons as a potential barrier and therefore serves as an electron "thermal barrier" between the end plugs and the solenoid. If we now heat the electrons in the plug with electron cyclotron resonant heating (ECRH) or other auxiliary heating, the final potential peak needed to plug up ions leaking from the solenoid can be generated with a much lower plasma density in the end plug relative to the density in the solenoid. It is this large reduction in plug density that is the advantage of thermal barriers.

A number of thermal-barrier configurations are under consideration. One, called the inside barrier, has the thermal barrier and the final potential peak in separate mirror regions, with that for the barrier on the inside (toward the central cell). The originally proposed barrier configuration[7] was an inside barrier, as was the conceptual reactor design presented in Ref. 7. The magnet arrangement for the latter design is shown in Fig. 1. Beginning at the central-cell end, we see the barrier coil (a solenoid), a transition coil to transform the magnetic flux bundle from circular to elliptical, the minimum-B plug coils (a yin-yang pair), and a circularizing coil. The latter optional coil is used to

recirculariza the elliptical flux bundle emerging from the yin-yang pair and permits the use of a direct converter with a circular cross section. The barrier region (potential depression) exists between the barrier coil and the yin-yang pair. The potential peak exists in the mirror region created within the yin-yang. The yin-yang pair also serves the purpose of providing the primary region of good magnetic field curvature essential for magnetohydrohynamic (MHD) stability. In this configuration, the magnetic field is unfavorably curved in the transition regions at the ends of the central cell, and therefore MHD stability places a limit on the plasma β in the central cell.

Another type of thermal-barrier configuration, called the A-cell barrier, is shown in Fig. 3. This configuration is the basis for the

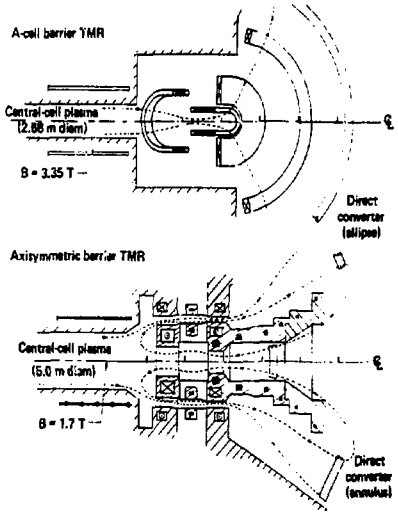

Fig. 3. A-cell barrier and axisymmetric-cusp barrier configurations.

MFTF-B design. The coil arrangement, looking outward from the central-cell solenoid, consists of a transition coil, a yin-yang pair, and a cee-shaped coil with the same orientation as the outer coil of the yin-yang pair. Two mirror cells are created, one within the yin-yang pair, the other between the yin-yang and the cee-coil. Both the thermal barrier and the final potential peak are created in the outer mirror cell, called the A-cell, whereas mirror-confined ions injected into the yin-yang cell serve mainly to provide MHD stability. As with the inside-barrier configuration, bad magnetic field curvature at the ends of the central cell places a limit on the plasma β in the central cell. To create the A-cell potential profile, the ions are injected away from the bottom of the magnetic well. Consequently, the injected ions slosh back and forth, creating peaks in density at their turning points, and application of ECRH to the outer density peak produces the final potential peak.

A third thermal-barrier configuration, called the axisymmetic cusp,[3] is also shown in Fig. 3. This configuration uses all circular coils. The coil arrangement, looking outward from the central-cell solenoid, consists of axially spaced pairs of concentric coils. The inner coil of each pair has current in the opposite sense from the central cell solenoid; the outer coil of each pair has current in the same sense. The resulting magnetic geometry has a point cusp on the machine axis encircled by a concentric ring cusp. Mirror regions--cylindrical on the axis with an encircling annular region--exist between the two primary pairs of concentric coils. (The middle pair of coils shown in Fig. 3 is for magnetic flux shaping.) The magnetic flux bundle threading the central cell maps through the annular mirror cell. A thermal barrier and a potential peak are created in each mirror region by an ECRH-heated, sloshing-ion distribution, just as in the A-cell of the previously discussed configuration. Unlike the inside- and A-cell barrier configurations, this configuration has good magnetic field curvature in the central cell, and MHD stability places no limit on the central-cell β. The β is limited to some value less than unity, however, to ensure alpha particle confinement.

A fourth proposed thermal-barrer configuration uses only simple mirror cells, produced by circular coils. MHD stability would be achieved by means of hot electron rings in the end plugs, as is done in the Elmo Bumpy Torus (EBT).

MHD Stability and Magnetic Field Design

MHD stability is a crucial issue for all the end plug-configurations described above. Lacking experimental data for any of these configurations, we must at this point rely on theoretical models to predict stability limits and thus to guide our comparative studies. The development of theoretical models to assess the interchange and ballooning modes of MHD stability for tandem mirrors with thermal barriers is a quite recent and still continuing endeavor.

Two models have been developed to separately assess interchange and ballooning stability for straight-axis tandem mirrors using minimum-B cells (this includes the inside- and A-cell barrier configurations). The interchange model uses the formula

$$\int ds \; \frac{P_{\perp} + P_{\parallel}}{B^2} \left(xx'' + yy''\right) > 0 \quad , \qquad (1)$$

where $p_\perp$, $p_\parallel$ are components of the pressure tensor; x,y are the off-axis loci of a field line and x",y" are the second derivatives (curvature) of x,y, with respect to s, the distance along the field line. The integral is taken over the full length of the tandem mirror machine. Equation (1) indicates that to the extent possible, regions of good (bad) curvature should be at high (low) pressure and low (high) field strength. The guidance on field line excursion from the axis is less clear since large excursions are a consequence of strong good curvature and in those good curvature regions make the integrand of Eq. (1) more positive, whereas large excursions become a penalty when the curvature goes bad. Thus we find an optimum amount of ellipticity or fanning in the minimum-B region. The interchange model has been found to establish necessary but not sufficient conditions for MHD stability. Because it is particularly simple and convenient to apply, it has proven to be a very useful tool for screening proposed coil designs.

Sufficient conditions for MHD stability are established by satisfying the more stringent requirements of ballooning. Ballooning at finite β allows an eigenfunction to localize in a region of bad curvature, but at the expense of requiring energy for field-line bending. The analytic model for assessing stability against ballooning is described in Ref. 6. Application of the model has shown that regions of good curvature do not compensate for far-away regions of bad curvature in ballooning as they do in interchange.

The inside-barrier magnet design presented in Ref. 7 more than satisfied the conditions for interchange stability at the desired high value for the peak, on-axis central-cell ($\beta_c > 0.5$), but application of the ballooning analysis indicated a maximum β_c value of only about 0.1. Because of this result, the emphesis at LLNL shifted to the A-cell barrier configuration, which was believed to have greater potential for ballooning stability at high β_c because the minimum-B "anchor" is closer to the region of bad magnetic curvature. (The A-cell configuration also has an apparent advantage concerning microstability, discussed in Ref. 6.)

Although A-cell barrier designs have yielded higher ballooning limits for β_c than the inside-barrier design, the determination of the maximum value achievable and an assessment of its adequacy for a power reactor are still incomplete. Table 1 gives a sample of calculated ballooning limits for β_c.

The Tandem Mirror Next Step (TMNS) design[9] is a preliminary conceptual design for the mirror machine to be built after MFTF-B. Both MFTF-B and TMNS are A-cell barrier configurations. The straight-bar model is an easily manipulated tandem mirror magnet design that includes a central-cell solenoid and minimum-B end plugs consisting of circular coils and straight Ioffe bar conductors. This model has no A-cell. (An important application of the straight bar-model was the investigation of the optimization of magnetic flux bundle ellipticity in minimum-B cells.[10]) In Table 1, B_{0p}, B_{mp}, and β_p are the central field, mirror field, and beta for the minimum-B cell, B_{0b}, and β_b are the barrier field and beta; and B_c is the central-cell field. The effect of lower B_c for TMNS, shown in the last line of Table 1, was predicted to follow $\beta_c B_c^2 =$ constant,[11] but was revealed by manipulations of the straight-bar model and the TMNS design to more closely follow $\beta_c B_c^{1.6} =$ constant. Reactor performance at lower B_c and higher β_c is discussed in the next section.

A theoretical model for ballooning stability for the axisymmetric cusp configuration is being developed. So far, results from this model are inconclusive, but it is clear that the limit will be on plug beta, not β_c. This is advantageous in that the fusion power is proportional to β_c^2, not to the plug beta squared. MHD stability considerations for the simple mirror tandem mirror with EBT rings have just begun.

Tandem Mirror Reactor Performance

Analytic physics models have been developed at LLNL and at the University of Wisconsin to predict plasma performance in tandem mirror fusion reactors with thermal barriers. Because of the rapidly evolving nature of the tandem mirror barrier concept, these models have undergone (and are still undergoing) a series of iterations.

Simply stated, the objective of physics model development is to provide a self-consistent set of equations, supported by

Table 1. MHD stability limits for β_c.

Magnet Design	B_{0p} (T)	B_{mp} (T)	B_{0b} (T)	B_c (T)	β_p	β_b	Balloon-limited β_c
MFTF-B	2.0	4.1	1.0	1.0	0.7	0.3	0.19
Straight bar model	6.0	9.0	-----	2.8	0.7	---	0.21
TMNS	6.0	9.0	1.7	2.5	0.7	0.3	0.30
TMNS with reduced B_c	6.0	9.0	1.7	1.6	0.7	0.3	0.57

physics theory and experiment, which can be used to calculate all of the plasma dimensions, densities, energies, potentials, and confinement times in a tandem mirror reactor. To be useful for parametric calculations, the model must be programmable for rapid solution by computer.

One physics model developed at LLNL for the inside-barrier configuration is described in Ref. 7. Example results from this model for a tandem mirror reactor producing 3500 MW of fusion power are presented in Ref. 12. For this study, the on-axis magnetic field strengths in the end-plug region were held fixed: 12 T at the position of the solenoidal barrier coil and 6 and 4 T at the yin-yang mirrors and midplane, respectively. The neutral beam injection energy was 400 keV. For a fixed first-wall neutron loading (1.3 MW/m^2) and several assumed values for central-cell β, the reactor was optimized to yield maximum plasma Q. A short table of results is shown in Table 2. Q was found to range from 11 to 18.

Table 2. Parameters for the LLNL Inside Barrier TMR

	Central Cell β		
	0.2	0.4	0.7
B_c, T (optimized)	4.4	2.8	2.1
r_c, m	1.0	1.3	1.6
L_c, m	280	220	170
Q	11	14	18

A similar plasma model for the inside-barrier configuration was developed at the University of Wisconsin.[13] This model includes an improved treatment of the relationship between plasma density, temperature, and potential, as motivated by Cohen's Fokker-Planck study.[14] Although this more accurate model predicts a decrease in performance, the decrease can be recovered through reoptimization and some increase in magnetic field strengths.

For all the inside-barrier examples given above, the β_c value has been assumed to be higher than the value predicted as the MHD stability limit for a particular coil design. (The prediction was $\beta_c \approx 0.1$ for a coil design with magnetic fields the same as those for the middle column of Table 2.) We do yet not know if higher β_c designs are possible for the inside-barrier configuration.

A series of physics models has been developed at LLNL to predict the plasma performance for tandem mirrors with the A-cell barrier configuration. The second generation of this series, consisting of scaling laws for each input power requirement based on the MFTF-B design point, was used to calculate the results given in this paper. A third-generation model, just being completed,[15] solves the detailed particle and energy balance equations as presented in Ref. 6.

Example results for an A-cell barrier TMR are shown in Fig. 4.[16] The figure shows

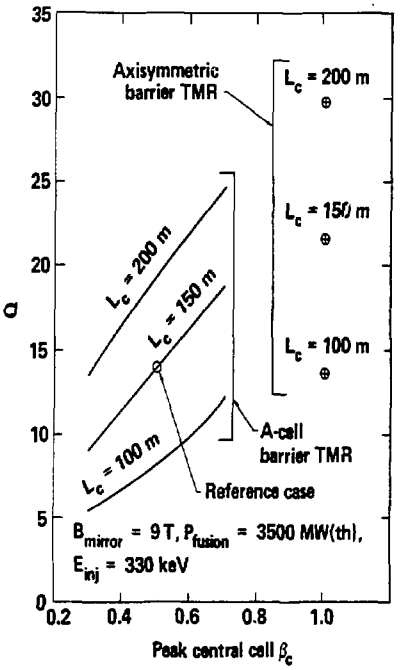

Fig. 4 Tandem reactor performance for A-cell barrier and axisymmetric cusp barrier configurations.

calculated plasma Q as a function of assumed peak (on-axis) β_c for several different central-cell lengths. In all cases, the fusion power is 3500 MW, the yin-yang mirror and center fields are 9 and 6 T, the A-cell mirror field is 9 T, the barrier minimum field is 1.7 T, and the yin-yang and barrier β values are 0.7 and 0.5, respectively. The other constraint for the A-cell cases of Fig. 4 is that the radius of the plug plasma was held constant at about 1 m. Consequently, along one of the constant L_c curves of Fig. 4, the central-cell magnetic field varies as $(1 - 0.6\beta_c)^{1/6}/\beta_c^{2/3}$, and the first-wall neutron loading varies as $(1 - 0.6\beta_c)^{1/3}/\beta_c^{1/3}$. (This scaling results from constant fusion power per unit length and magnetic flux conservation; the 0.6 factor comes from profile-averaging β_c, which is the peak, on-axis beta value.) The values for central-cell field and first-wall loading at the reference point identified on the figure are 3.4 T and 1.9 MW/m^2, respectively.

Coincidentally, the β_c, B_c relationship along the constant L_c curves of Fig. 4 is very close to $\beta_c B_c^{1.6}$ = constant, which was found in the MHD study to be a condition for constant stability. Thus, we would expect each constant L_c curve to be either stable or unstable in its entirety. Unfortunately, for coil designs we have devised to date, our predictions are that the A-cell configuration curves of Fig. 4 are unstable. Comparing the reference case to Table 1, for example, indicates that we would have to reduce the central-cell field to about 1.6 T to achieve a stable β_c value of 0.5 to 0.6.

Reducing B_c to achieve stability results in an increase in the plasma radii if L_c and fusion power are held constant. For example, taking the reference case of Fig. 4, reducing B_c to 1.5 T, and estimating a stable β_c of 0.6 results in an increase in plug plasma radius from 1.0 to 2.7 m. The central-cell plasma radius increases by an even greater ratio, from 1.3 to 5.3 m, resulting in a decrease in first wall-neutron loading from 1.9 to only 0.5 MW/m^2. Calculations show that the plasma Q decreases from 14 to 11. Thus, although we can identify a specific A-cell magnetic design predicted to be MHD stable and yielding a reactor with $Q > 10$, the fusion power density is perhaps uneconomically low. Work is continuing to more firmly establish the limits of the A-cell configuration.

Figure 4 also shows some preliminary results for TMR's with the axisymmetric-cusp end-plug configuration. (These results were calculated using a model similar in detail to the second-generation model for the A-cell configuration.) The axisymmetric-cusp cases have the same fusion power and plug mirror fields (9 T) as the A-cell cases. Higher Q's are expected with the axisymmetric cusp because of the near-unity peak beta achievable in the central cell. Note that the axisymmetric results are somewhat below the extrapolation of the A-cell curves; this is because of the additional plug plasma volume in the axisymmetric configuration (the on-axis plug volume which does not flux map to the central cell). Verification of these preliminary results for the axisymmetric-cusp configuration awaits the completion of the MHD stability analysis.

End-Plug Technologies

The detailed design of end-plug components for a tandem mirror reactor with thermal barriers must await the choice of end-plug configuration. However, there is enough similarity among the various configurations that the general end plug technological requirements can be discussed. The end-plug technologies include high-field superconducting magnets, neutral beam injectors, and gyrotrons for (ECRH).

Superconducting Magnets

Both the inside-barrier and A-cell barrier configurations require minimum-B mirror cells such as those produced by yin-yang magnets. The minimum-B cells for the inside-barrier cases we considered had mirror and central fields of 6 and 4 T (LLNL design), and 9 and 6 T(University of Wisconsin design), respectively, while the A-cell cases all had fields of 9 and 6 T. These field values are all for vacuum fields on-axis. Carefully designed yin-yang magnets can achieve coil efficiencies (maximum on-axis field divided by peak conductor field) of about 0.75. Thus, the peak conductor fields of interest are 8 or 12 T. The first can be done with Nb-Ti superconductor; the second requires the less developed superconductor, Nb_3Sn.

The structural support of large, high-field yin-yang coils is a difficult engineering problem. A study by Grumman Aerospace Corporation [17] has demonstrated that the support of reactor-sized yin-yang coils with peak conductor fields of 8 or 9 T is feasible with thick-walled magnet cases and intercoil bracing (similar to the support structure methods used on the MFTF yin-yangs magnet). For the 12 T yin-yang magnets specified for the A-cell configuration, it appears that massive external clamping structures will be required.

Circular coils, such as those required for the barrier coil of the inside-barrier configuration and for all of the coils of the axisymmetric-cusp and simple mirror configurations, are much more easily designed than yin-yang coils, because most of the electromagnetic forces can be taken as simple hoop forces.

Neutral Beam Injectors

Neutral beam injectors are proposed for two different purposes in tandem mirror reactors with thermal barriers: sustenance of the end-plug plasma and charge-exchange pumping of the barrier region. All neutral beam injectors must operate continuously.

Although the introduction of direct electron heating and thermal barriers has reduced the necessary plug-plasma neutral beam injection energy from the 1.2 MeV specified in Ref. 3, the energy requirement is still in the 100's of keV. This is because the plug ions injected at the potential peak are in trapped velocity space only if

$$E_{inj} > \frac{\phi_c + \phi_e}{R - 1} ,$$

where $\phi_c + \phi_e$ is the height of the potential

peak (see Fig. 2) and R is the ratio of the magnetic field strength at the mirror point to that at the injection point. As an example, the LLNL inside-barrier TMR with $\beta_c = 0.4$ (middle column of Table 2) had $\phi_c + \phi_e = 265$ keV and R = 1.9; therefore the minimum plug injection energy was 295 keV. The design used 400-keV injection. The A-cell examples of Fig. 4 had E_{inj} = 100 keV in the yin-yang cell and 330 keV in the A-cell. We prefer the negative-ion type neutral beam injector for the TMR plugs because of its efficiency at the required energies is higher that that possible with positive-ion-type injectors.

For all thermal barrier configurations, it is necessary to pump away trapped ions accumulating in the barrier as a result of collisions among ions passing back and forth from the central cell. Such filling is unacceptable because it would negate the depression in plasma potential. It has been proposed (and will be tested experimentally on TMX Upgrade and MFTF-B) that the pumping can be accomplished by having the trapped ions undergo charge-exchange interactions with neutral beams located at each end of the machine and aimed nearly along the axis. In a charge-exchange collision between a trapped ion and an axially aimed neutral, a trapped ion is exchanged for one that is not trapped. An advantage of this pumping method is that it is based upon well understood, classical processes. Possible disadvantages are that access for axial injection may be difficult, and various inefficiences may hurt the power balance. Other approaches to ion pumping in thermal barriers will also be explored in the tandem mirror physics program.

Analysis of the charge-exchange pumping concept has shown that to minimize the power requirements for the pump beams a multistage pumping system is desirable. In this system, decreasing fractions of the total ion load are pumped by injectors of increasing energy level (a situation analogous to a multistage vacuum pumping system in which decreasing fractions of the total gas load are pumped at increasing vacuum levels).

Reference 7 describes the methodology behind the design of a four-stage barrier pump system for an inside-barrier TMR. The system consists of a gas jet to charge exchange with those trapped ions that follow drift surfaces extending out of the main plasma column, and neutral beams at three energies: 10, 50, and 139 keV. The specific system described required a total injection current nearly double the required pumping rate, largely because of the competing ionization reactions. (An ionization reaction provides a fuel ion to the central cell, but does not remove a trapped ion.)

An important extra function of the charge-exchange pumping system might be the removal of thermalized alpha particles from the reactor.[16] Under certain conditions, the charge-exchange reaction $He^{++} + D^0 \rightarrow He^+ + D^+$ will lead to the loss of the He^+ ions over the potential peak. Preliminary estimates are that this ash-removal scheme can adequately restrict the accumulation of alpha particles, thereby making possible steady-state reactor operation.

Negative-ion-type neutral beam injectors are preferred for charge-exchange pumping for two important reasons. First, for the high-energy pump beam, negative ions are desired for the usual reason of neutralization efficiency. The second reason is the normal presence of positive molecular ions in positive-ion-type sources, which produce atoms with 1/2 or 1/3 of the primary beam energy. The fractional energy components are undesirable in any neutral beam but are intolerable in a charge-exchange beam if they become trapped in the barrier potential well.

Electron Heating

Electron heating in the plug region is an important element of reactor design for TMR's with thermal barriers. We propose to accomplish the electron heating with radio-frequency sources (rf) sources operating in the ECRH regime (30 to 150 GHz). Efficient transfer of rf power to plasma heating normally requires coupling with one of the fundamental plasma resonances. In ECRH, the resonant frequency is the fundamental or a harmonic of the electron cyclotron frequency; i.e..

$$f = nf_{ce} = neB/2\,m_e = 28Bn, \qquad (2)$$

where n is the harmonic number, f is in GHz, and B is in teslas. however, the resonant condition must occur where the plasma is accessible to the injected rf power. This requires that the microwave frequency be higher than the electron plasma frequency to avoid reflections from the plasma cutoff; i.e.,

$$f > f_{pe} = (1/2\pi)(n_e e^2/m_e \varepsilon_0)^{1/2} = 9.98 \times 10^{-6} n_e^{1/2}, \qquad (3)$$

where f_{pe} is in GHz and n_e is in cm^{-3}. Combining Eqs. (2) and (1) yields the requirement

$$\frac{nB}{n_e^{1/2}} > 3.21 \times 10^{-7}. \qquad (4)$$

Fortunately, TMR plug parameters typically satisfy Eq. (4) for all harmonics. The recent and continuing development of gyrotron oscillators has improved the feasibility of ECRH at the frequencies and power levels required for

TMR's (10's of MW at 30 to 150 GHz).

Central Cell Design

In the TMR, the fusion power is produced in the cylindrical-geometry central cell. The design goal for the central cell is that it be compact, simple to fabricate using mass production techniques, and easily maintained. Fortunately, the central cell is largely decoupled from the plug regions, and its design can be optimized somewhat independently of the complexities of the end plugs.

A basic design philosophy adopted for the TMR central cell is that of axial modularity, as depicted in Fig. 5. The central cell is divided

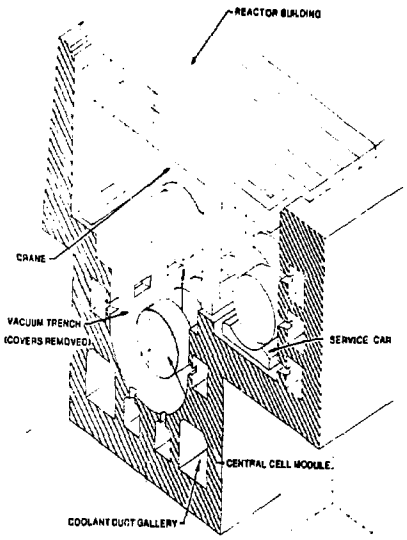

Fig. 5 Central cell of tandem mirror reactor.

into cylindrical modules, typically 2 m in length and 8 m in outside diameter. The modules, each containing blanket, shield, and two solenoidal magnets, can be individually removed by crane for service or replacement. As a design variation, the removable module might consist of only blanket and shield if the magnet segments can be moved axially to provide adequate space for module withdrawal.

The central cell must have some way to provide high-vacuum conditions in the plasma region; at the same time, however, easy module separation is an advantage for maintenance. One possibility is to house the entire central cell in a vacuum trench maintained at 10^{-2} Torr, and to achieve high vacuum in the plasma region through the use of pressurized-cushion seals between modules. The cushion seals are of annular shape and have a radial dimension of 1 m (the shield thickness). The cushion seal uses omega-joint expansion elements, that behave similarly to a bellows but are much more rugged (see Fig. 6). One cm of clearance for assembly can be obtained by evacuating the cushion to allow the ambient pressure in the trench to collapse it. (Though normally evacuated, the trench is backfilled to atmospheric pressure with dry air or inert gas prior to the beginning of a module change-over.) The two faces of the cushion are contoured on their inner surfaces (in contact with the pressure energizing fluid) to impede neutron leakage.

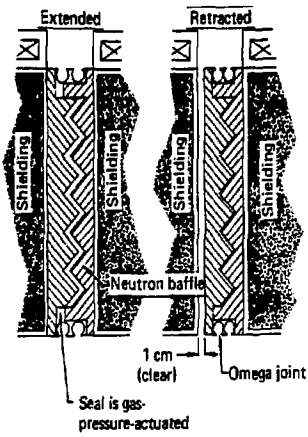

Fig. 6 Central cell module-to-module pressurized cushion seal.

Many different designs are possible for the central-cell modules. The example discussed here is a pod design using solid lithium oxide as a neutron moderator and tritium breeder and helium as a coolant. An alternative design by the University of Wisconsin uses liquid lithium lead as moderator, tritium breeder, and coolant.[13] Figure 7 shows three central-cell modules of the pod type, as designed at LLNL. The central-cell solenoidal coils are at the periphery of the modules. Because typical central cell fields strengths are 2 to 3 T the coils are constructed of Nb-Ti superconductor. Just inside the coils is the shield region. The shield is made of poured lead concrete in a steel case. Inside the shield region is the blanket. The blanket comprises 2 m-long pods, arranged in parallel to the machine axis, and grouped together into pod clusters, each of which has a common coolant gas distributor. Each pod is a 25-cm-diam cylinder with hemispherical ends, and is constructed of Inconel 718*. The pod contains a cylindrical stainless steel canister of lithium oxide

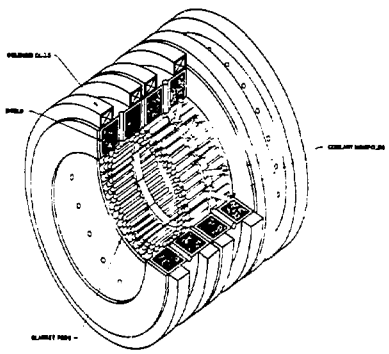

Fig. 7 Pod type central cell modules.

granules. The canister is penetrated by longitudinal tubes, also of stainless-steel. The helium coolant flow path is as follows: the coolant enters via an inlet pipe inside a stem piercing the shield (see Fig. 7), flows through one side of the gas distributor and is divided among the pods, flows from the midplane of the pod to both ends between the pod wall and the inside canister, returns to the pod midplane through the canister tubes, collects in the other side of the gas distributor, and exits via an outlet pipe in the stem. The helium inlet temperature is 350°C; outlet temperature is 550°C.

References

1. T.K. Fowler and B.G. Logan, "The Tandem Mirror Reactor," Comments Plasma Phys. 2, 167 (1977).

2. G.I. Dimov, V.V. Zakaidakov, and M.E. Kishinevshy, "Open Trap With Ambipolar Mirrors," Fiz. Plasmy 2, 597 (1976).

3. R. W. Moir, W. L. Barr, G. A. Carlson, W. L. Dexter, J. N. Doggett, J. H. Fink, G. W. Hamilton, J. D. Lee, B. G. Logan, W. S. Neef, Jr., M. A. Peterson, and M. E. Rensink, Preliminary Design Study of the Tandem Mirror Reactor, Lawrence Livermore Laboratory, Livermore, CA, UCRL-52302 (1977).

4. D. E. Baldwin, B. G. Logan, and T. K. Fowler, An Improved Tandem Mirror Fusion Reactor, Lawrence Livermore Laboratory, Livermore, CA, UCID-18156 (1979).

5. F. H. Coensgen, T. C. Simonen, A. K. Chargin, and B. G. Logan, TMX Upgrade Major Project Proposal, Lawrence Livermore National Laboratory, Livermore, CA, LLL-POP-172 (1980).

6. D. E. Baldwin, B. G. Logan, T. C. Simonen (Editors), Physics Basis for MFTF-B, Lawrence Livermore National Laboratory, Livermore, CA, UCID-18496-Parts 1 and 2 (1980). See also K. I. Thomassen, and V. N. Karpenko, Tandem Mirror Fusion Test Facility, MFTF-B, LLL Report Lawrence Livermore National Laboratory, Livermore, CA LLL-POP-163, Rev.1, (1980).

7. G. A. Carlson, B. Arfin, W. L. Barr, B. M. Boghosian, J. L. Erickson, J. H. Fink, G. W. Hamilton, B. G. Logan, J. O. Myall, and W. S. Neef, Jr., Tandem Mirror Reactor with Thermal Barriers, Lawrence Livermore National Laboratory, Livermore, CA, UCRL-52836 (1979).

8. B. G. Logan, An Axisymmetric, High Beta Tandem Mirror Reactor, Lawrence Livermore Laboratory, Livermore, CA, UCRL-83555 (1979).

9. J.N. Doggett, C.C. Damm, R.H. Bulmer, W.S. Neef, G.W. Hamilton, A.E. Sherwood, S. Szybalski, B.M. Boghosian, G.A. Carlson, R.W. Moir, W.L. Barr, J.L. Erickson, R. W. Devoto, T.H. Batzer, "The Tandem Mirror Next Step Conceptual Design", these Proceedings.

10. J. Myall, The Use of a Simple Quadrupole Magnet Model for MHD Stability Calculations in a Tandem Mirror Reactor, Lawrence Livermore National Laboratory, Livermore, CA, UCID-18720 (1980).

11. D. E. Baldwin, Lawrence Livermore National Laboratory, Livermore, CA, personal communication (1980).

12. B. M. Boghosian, D. A. Lappa, and B. G. Logan, Physics Parameter Calculations for a Tandem Mirror Reactor with Thermal Barriers, Lawrence Livermore Laboratory, Livermore, CA, UCID-18314 (1979).

13. B. Badger, J. B. Beyer, J. D. Callen, R. W. Conn, G. A. Emmert, S. Grotz, S.O. Hong, J. Kesner, G. L. Kulcinski, L. L. Lao, D. C. Larbalestier, E. Larsen, L. P. Mai, T. K. Mau, C. W. Maynard, I. Ojalvo, K. Okula, M. Ortman, R. Perry, J. Santarius, J. Scharer, K. Shaing, I. Sviatoslavsky, D. K. Sze, W. F. Vogelsang, A. White, and P. Wilkes, Preliminary Information on the University of Wisconsin Tandem Mirror Reactor Design, University of Wisconsin, Madison, WI, UWFDM-325 (1979).

14. D. E. Baldwin, R. H. Cohen, T. A. Cutler, T. B. Kaiser, B. G. Logan, Y. Matsuda, A. A.

* Reference to a company or product name does not imply approval or recommendation of the product by the University of California or the U.S. Department of Energy to the exclusion of others that may be suitable.

Mirin, L. D. Pearlstein, M. Porkolab, M. E. Rensink, and T. D. Rognlien, Studies in Tandem Mirror Theory, Lawrence Livermore National Laboratory, Livermore, CA, UCRL-83519, Rev. 1 (1980).

15. B.M. Boghosian, "Plasma Performance Study for the Tandem Mirror Reactor", these Proceedings.

16. B. G. Logan, B. Arfin, W. L. Barr, B. M. Boghosian, G. A. Carlson, T. C. Chu, J. L. Erickson, J. H. Fink, T. K. Fowler, G. W. Hamilton, T. Kaiser, R. W. Moir, J. O. Myall, W. S. Neef, Jr., R. W. Conn, G. A. Emmert, F. Kantrowitz, J. Kesner, L. L. Lao, J. Santarius, and K. S. Shaing, Tandem Mirror Reactors with Thermal Barriers, Lawrence Livermore National Laboratory, Livermore, CA, UCRL-83505 (1980).

17. J.L. Erickson, I.U. Ojalvo, and J.O. Myall, "Structural Support of a Yin-Yang Magnet for a Tandem Mirror Reactor with Thermal Barriers", these Proceedings.